A Practical Solution for Torsional Vibrations Evasion in Variable Speed Drives

Khaled ElShawarby, Roberto Perini,
Giovanni M. Foglia, Antonino Di Gerlando
DENG
Politecnico di Milano
Milan, Italy
{khaled.elshawarby, roberto.perini
gianmaria.foglia, antonino.digerlando} @polimi.it

Mattia Rossi, Francesco Castelli Dezza
DMEC
Politecnico di Milano
Milan, Italy
{mattia.rossi, francesco.castellidezza}@polimi.it

***Abstract*—The paper presents a practical solution for an existing drive-train to avoid torsional vibrations for variable speed drives under SPWM modulation technique. Torsional natural frequencies can be a problem because either ill defined in design stage or one of the mechanical parameters has changed after the initial design stage. The proposed method comprises of dividing the frequency range into several partitions where in each partition a value of modulation frequency ratio m_f is chosen. A criterion is developed to choose m_f based on avoiding torsional excitations with the minimum converter losses. Torque harmonic distortion and converter losses are analyzed. Matlab/Simulink is used to validate the approach.**

***Index Terms*—Torsional Vibrations, Variable Speed Drives, Sinusoidal Pulse Width Modulation (SPWM).**

I. Introduction

One of the technical challenges associated with electric machines driven by power electronics converters is the mitigation of torsional vibrations. Torsional resonances occur for any drive-train; even simple drive trains consisting of a motor driving a load have at least one torsional mode. Converter modulation techniques generate torque harmonics which subsequently excite the natural resonance frequency of the drive-train. Torque harmonics amplitudes as low as 1% of the rated torque can be dangerous [1]. Torsional vibrations is even a bigger concern for high power applications thus various mitigation techniques have been studied [2]–[7].

This paper proposes a practical solution to avoid torsional vibrations in variable speed existing applications, also maintaining low switching losses and better quality waveforms. The principle of changing modulation frequency ratio m_f for each frequency range is a well known concept in the literature. The proposal is to use it to eliminate torsional vibration problems.

Wind Energy Conversion Systems (WECSs) can be suited for this kind of approach because wind power harvesting is achieved in a defined wind speed range namely from cut-in speed $V_{w,cut-in}$ up to the rated speed $V_{w,rated}$ as shown in Fig. 1. Thus, a starting frequency ratio m_{fo} can be of a value high enough in a way that no critical points can be excited. Since the dynamical phenomenon involved in WECSs application is slow, the operating frequency range can be divided into portions: in each portion a selected m_f is chosen. The criteria of selecting m_f can be simplified into two points:

- avoiding critical frequencies excitation;
- keeping switching frequency fixed in a certain range, i.e. limited switching losses.

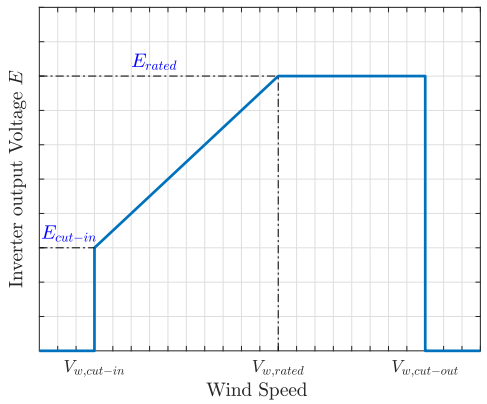

Fig. 1. Typical wind energy converter output voltage. The converter harnesses power from $V_{w,cut-in}$ to $V_{w,cut-out}$, where the linear range ($V_{w,cut-in}$ to $V_{w,rated}$) is run usually under MPPT conditions.

The rest of this work is organized as follows. Section II defines the method to divide the frequency regions and the choice of m_f with respect to torsional vibrations excitation. Section III introduces the system to be studied, focuses on the mechanical assembly, defining the torsional natural frequencies. Section IV derives the approximated expression of the electromagnetic torque for SPWM modulation. Section V analyzes the converter losses and the torque total harmonic distortion for the proposed method. Section VI presents simulations results of the proposed technique.

II. Frequency range definition and criteria to choose m_f

A. Criteria to choose m_f

The choice of m_f is based on avoiding torsional vibrations excitation keeping m_f odd and multiple of three. In

order to avoid critical points, a Campbell diagram should be considered. It describes the relation between electrical harmonic excitations versus the torsional natural frequencies. The intersections between a harmonic frequency and one of the torsional natural frequencies TNF_i represent the so called critical point i.e. torsional resonance occurrence. A critical frequency f_{cr} can be found by dividing TNF_i by a random harmonic h.

Considering Sinusoidal PWM (SPWM) technique, according to the analysis performed in [8] for the electromagnetic torques, the least order harmonic present $h = m_f - 3$. In order to avoid the harmonic excitation, m_f can be calculated as:

$$m_f \geq \frac{TNF_{max}}{f_{limit}} + 3 \tag{1}$$

where f_{limit} is the lowest starting frequency to avoid critical points (critical points occur for frequenices lower than f_{limit}). In order to keep low switching losses, (1) has to be minimized keeping m_f odd and multiple of three.

B. Frequency Range Definition

Thus, in order to avoid the torsional vibrations excitations, it is enough to set f_{limit} equal to f_{cut-in} and evaluate m_f accordingly. However, it is not necessary to operate at high switching frequencies (i.e. higher converter losses) for a wide frequency range. Thus, a way can be dividing the speed range into partitions in which each partition lower frequency will be a new f_{limit} entailing a new value of m_f.

There can be several aspects to consider in how to divide the operating range of a certain application since it depends on the application itself. As for WECSs application, the idea is to divide the frequency range, based on the frequency of occurrence, as shown in Fig. 2 into three portions:

- near cut-in frequency region ($f_{cut-in} - f_{limit_1}$);
- an intermediate frequency region ($f_{limit_1} - f_{limit_2}$);
- near rated frequency region ($f_{limit_2} - f_{rated}$).

It has to be noted that, if the working frequency is fluctuating around a border frequency limit f_{limit_n}, m_f will fluctuate as well between two values. Thus, some constraints have to be set in order to avoid such condition:

- changing m_f according to a tolerance band;
- changing m_f if the frequency stabilizes for a given time.

Some additional constraints can be considered to the evasion of torsional vibration as a defined maximum level of converter losses or a maximum value of the total harmonic distortion THD. In such a case, the frequency range should be divided into smaller portions where for each of them a new m_f is chosen. However, the number of transients will increase due to the frequent change of m_f.

III. Mechanical Assembly

Consider a three-modules Axial Flux Permanent Magnet Synchronous Generator (AFPMSG) drive train as shown in Fig. 3 whose data are reported in Table I. The AFPMSG is directly driven (DD) by a wind turbine whose inertia is

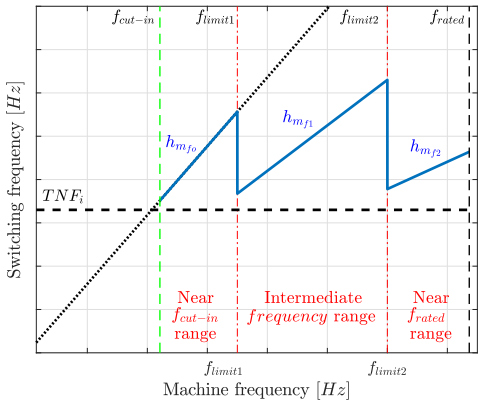

Fig. 2. Campbell diagram for the proposed method of dividing the frequency range into portions: Near f_{cut-in} - Intermediate frequency - Near f_{rated} ranges, against operating with m_f high enough to avoid TNF_i. In each region m_f decreases, i.e. the corresponding harmonic h has a lower slope.

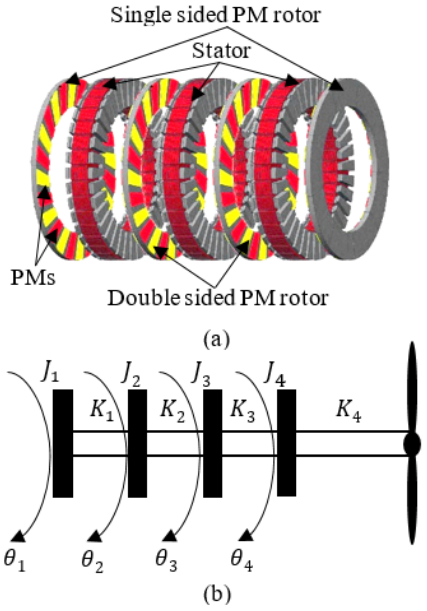

Fig. 3. (a) Three-module AFPMSG consists of three stators and four rotors where the outer rotor disks (J_1, J_4) are single-sided PM rotors, while both middle rotor disks (J_2, J_3) are double sided PM rotors (b) Mechanical equivalent model for the machine connected to the wind turbine.

much higher than any of the machine rotors. Thus, the angular deflection of the turbine is assumed to be zero.

Using the well known eigen-values approach, natural frequencies can be calculated by equating the Newton's equations to zero. Assuming Simple harmonic motion and neglecting the internal damping, the mechanical system of equations can be written as:

$$\left((2\pi * \{TNF\})^2 \left[J\right] + \left[K\right] \right) * \left[\theta\right] = \{0\} \tag{2}$$

where TNF is a vector of the torsional natural frequencies of the mechanical assembly. $\left[J\right]$ is a diagonal matrix of the moments of inertia of the rotors: J_1 and J_4 are both single-

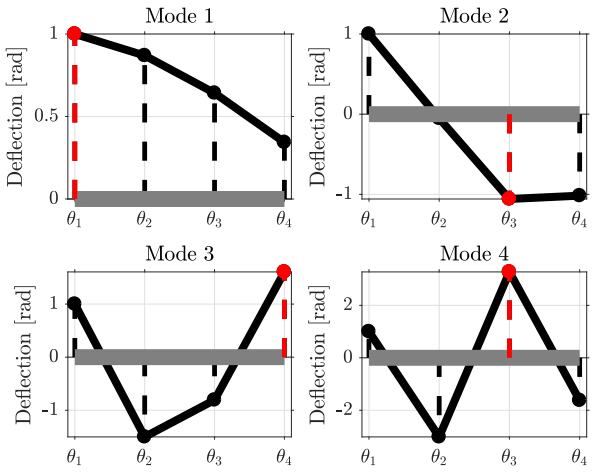

Fig. 4. Angular deflection of each rotor with respect to each mode of vibration. The angular deflection θ_1 is taken as a reference $\theta_1 = 1$ [rad]. The maximum angular deflection for each mode is highlighted in red which will be used in the following analysis.

sided permanent magnets (PMs) rotors while J_2 and J_3 are double-sided PMs rotors. $[K]$ is the stiffness matrix and is given by:

$$[K] = \begin{bmatrix} K_1 & -K_1 & 0 & 0 \\ -K_1 & K_1+K_2 & -K_2 & 0 \\ 0 & -K_2 & K_2+K_3 & -K_3 \\ 0 & 0 & -K_3 & K_3+K_4 \end{bmatrix} \quad (3)$$

where each individual stiffness is calculated using the classical De Saint Venant's principles. The values are verified to be an accurate approximation compared to the values obtained from Finite Element Method (FEM) with ANSYS Mechanical. $[\theta]$ is the vector of angular deflection of the four rotors. The shaft portion between the machine and turbine K_4 is assumed to have the same stiffness as the one of the internal machine shaft portions.

Thus, solving (2), the natural frequencies of the system are:

$$TNF = \begin{Bmatrix} 239 \\ 679 \\ 1047 \\ 1326 \end{Bmatrix} \text{[Hz]}$$

Each Natural frequency corresponds to a mode of vibration as shown in Fig. 4. However, the lower modes of vibrations are always more critical with respect to higher modes due to their low inherent damping. Thus, for the purpose of the analysis, only the first and second modes are taken into account.

IV. Electric Excitations due to SPWM

An approximate mathematical expression was provided in [7], which accurately calculates the electromagnetic torque (T_e) harmonic amplitudes due to the SPWM modulation. The torsional vibrations in AFPMSG is a local phenomenon occurring on the shaft connecting two rotors. Thus, the considered

TABLE I
SINGLE MODULE AXIAL FLUX PERMANENT MAGNET MACHINE NAMEPLATE DATA

P_n [MW], I_n [A]	1.0 , 713
Rated frequency f_{rated} [Hz], Rated Speed Ω_n [rpm]	14.73, 17
Line to neutral EMF at rated speed [V] (sinusoidal waveform)	435
Phase resistance R [mΩ]	14.59
Synchronous inductance (d,q axes) L [mH]	4.321
Rotor ext. diameter R_{ext}, Axial length [m]	5.00, 0.603
Hollow shaft stiffness K [Nm/rad]	$8.93 * 10^{11}$
Single-sided PM rotors inertias J_1, J_4 [kgm^2]	$5.17 * 10^4$
Double-sided PM rotors inertias J_2, J_3 [kgm^2]	$4.4 * 10^4$
Turbine inertia [kgm^2]	$3 * 10^6$
No damping cage	

T_e is the one T_{e_μ} produced by each module μ of the machine .

$$T_{e_\mu} = \frac{\sqrt{3} * p * \psi_{PM}}{2} i_{q_\mu} \quad (4)$$

where, p is the number of poles, ψ_{PM} is the PM flux and i_{q_μ} is the μ-th module quadrature current, which is given by (5).

$$\begin{aligned} i_{q\mu}(t) = \sqrt{\frac{3}{2}} \cdot \Bigg[& I_1 \sin\left(\phi + \delta - \frac{\pi}{2}\right) \\ & + I_{m_f-4} \sin\left((m_f-3)\,\omega_o\,t + \delta - \theta_{m_f-4} - \frac{\pi}{2}\right) \\ & - I_{m_f-2} \sin\left((m_f-3)\,\omega_o\,t - \delta - \theta_{m_f-2} + \frac{\pi}{2}\right) \\ & + I_{m_f+2} \sin\left((m_f+3)\,\omega_o\,t + \delta - \theta_{m_f+2} - \frac{\pi}{2}\right) \\ & - I_{m_f+4} \sin\left((m_f+3)\,\omega_o\,t - \delta - \theta_{m_f+4} + \frac{\pi}{2}\right) \\ & + I_{2m_f-1} \sin\left((2m_f)\,\omega_o\,t + \delta - \theta_{2m_f-1} - \frac{\pi}{2}\right) \\ & - I_{2m_f+1} \sin\left((2m_f)\,\omega_o\,t - \delta - \theta_{2m_f+1} + \frac{\pi}{2}\right) \\ & + I_{3m_f-4} \sin\left((3m_f-3)\,\omega_o\,t + \delta - \theta_{3m_f-4} - \frac{\pi}{2}\right) \\ & - I_{3m_f-2} \sin\left((3m_f-3)\,\omega_o\,t - \delta - \theta_{3m_f-2} + \frac{\pi}{2}\right) \\ & + I_{3m_f+2} \sin\left((3m_f+3)\,\omega_o\,t + \delta - \theta_{3m_f+2} - \frac{\pi}{2}\right) \\ & - I_{3m_f+4} \sin\left((3m_f+3)\,\omega_o\,t - \delta - \theta_{3m_f+4} + \frac{\pi}{2}\right) \\ & + I_{4m_f-1} \sin\left((4m_f)\,\omega_o\,t + \delta - \theta_{4m_f-1} - \frac{\pi}{2}\right) \\ & - I_{4m_f+1} \sin\left((4m_f)\,\omega_o\,t - \delta - \theta_{4m_f+1} + \frac{\pi}{2}\right) \Bigg] \end{aligned} \quad (5)$$

where, I_h is the current harmonic amplitude, ϕ the displacement between voltage and current fundamental components, δ the load angle, m_f the SPWM frequency modulation ratio, ω_o the output fundamental angular frequency. The voltage and current harmonic amplitudes and characteristic angles, I_h and θ_h, are obtained by applying each voltage harmonic, calculated in [8], to the equivalent $R-L-e$ circuit of the AFPMSG.

TABLE II
VALUES OF m_f WHICH AVOIDS THE NATURAL RESONANCES FOR BOTH TNF_1 AND TNF_2

	$f_{cut_{in}}$ to f_{limit_1}	$f_{limit_1} - f_{limit_2}$	$f_{limit_2} - f_{rated}$
$m_{f,TNF1}$	63	39	27
$m_{f,TNF2}$	159	105	63

From (4) and (5), the torque THD for the μ-th module $THD_{T\mu}$ can be evaluated; it is evident the dependence $THD_{T\mu}$ on the ac current harmonic amplitudes I_h.

V. HARMONIC DISTORTION AND CONVERTER LOSSES ANALYSIS

The proposed method is mainly focused on avoiding TNF excitations and on dividing the frequency range into portions in order to decrease m_f. Basically that has consequences on the converter losses and THD_T. Assuming f_{cut-in} = $0.3 \cdot f_{rated}$ = 4.42 Hz, the limit frequencies are assumed to be 7.5 and 11.5 Hz, then two cases are considered: the former avoids the excitation of the TNF_1, while the latter avoids the excitation of both TNF_1 and TNF_2. For each case the values of m_f are calculated by choosing the first odd m_f and multiple of three satisfying (1) and are labeled as $m_{f,TNF1}$ and $m_{f,TNF2}$.

Fig. 5 shows the Campbell diagram for $m_{f,TNF1}$ and $m_{f,TNF2}$. In particular the least order harmonic $m_f - 3$ is plotted for each frequency range. It can be seen no critical points are excited for the targeted TNF.It has to be noted that only $m_f - 3$ are plotted which means higher order harmonics will probably excite higher modes. As an example, Fig. 6 shows the effect of high order harmonics for $m_{f,TNF1}$ on $TNF2$. It shows the harmonic $2m_f$ exciting TNF_2 in each frequency partition, i.e. three critical frequencies arise (f_{cr1}, f_{cr2}, f_{cr3}). The amplitudes of the angular deflection due to vibrations depend on the amplitude of the exciting torque and the internal damping of the system. Thus, it has to be verified that the excitation of these critical points does not cause problems for the system.

Fig. 7 shows the effect of such a combination of m_f values on the THD_T. Two issues are apparent [8], [7]: if m_f increases, the harmonic order h increases, and the harmonic amplitude I_h decreases according to (6)

$$I_h = \frac{V_h}{Z_h} = \frac{V_h}{\sqrt{R^2 + (h \cdot \omega_o \cdot L)^2}} \tag{6}$$

where, V_h and Z_h are the harmonic voltages and characteristic impedances respectively. As mentioned earlier, $THD_T \propto I_h$, Therefore, $THD_T \propto {m_f}^{-1}$. Moreover, at low frequencies, the THD_T increases as the weight of the harmonics to the fundamental increases.

The used converter comprises of six IGBTs where the total converter losses (P_{total}) can be split into conduction and commutation losses. Conduction losses occur in the diodes and transistors and are denoted by P_D and P_T respectively. While transistor commutation losses are function of the switching frequency and denoted by P_{COM}. For SPWM modulation the

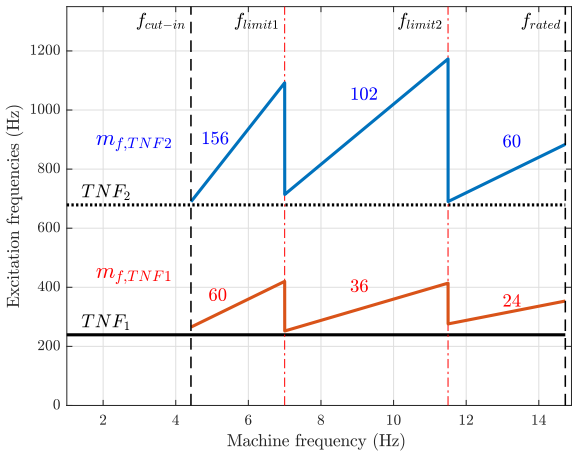

Fig. 5. Campbell Diagram for the proposed method to avoid TNF_1 (solid) and TNF_2 (dotted). The only harmonic shown is the least $m_f - 3$. It can be seen there are no critical points excited, i.e. no resonance occurs.

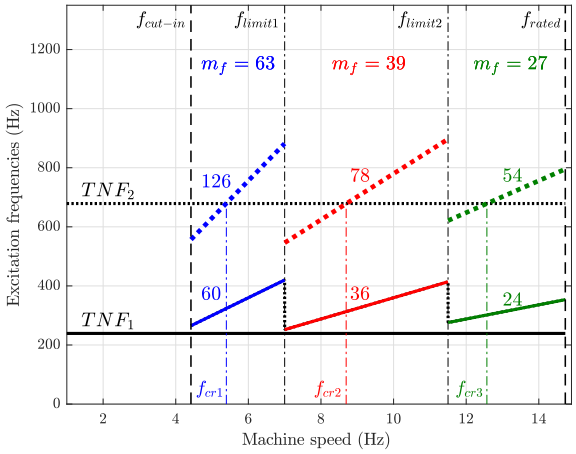

Fig. 6. The Campbell diagram of the proposed method adopting the first TNF as a reference to avoid. As it can be seen some critical points arises from the intersection of the harmonic $2m_f$ with the second TNF

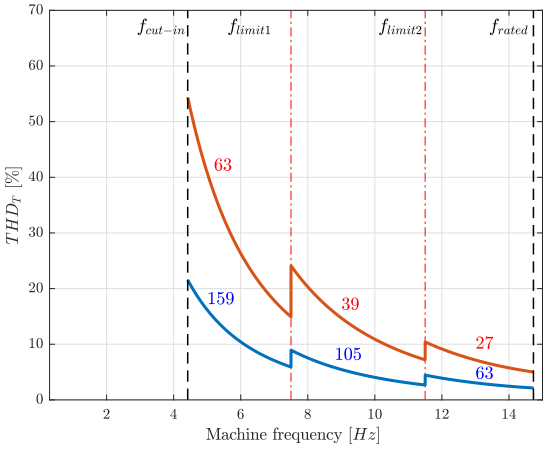

Fig. 7. THD_T for the proposed method to avoid TNF_1 and TNF_2. Using higher values of m_f has lower values of the harmonic distortion.

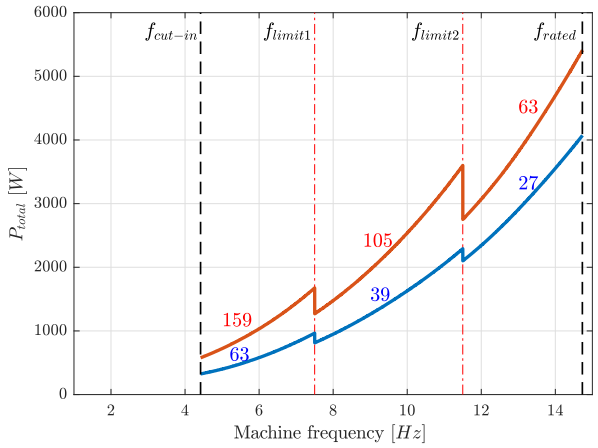

Fig. 8. Single module converter losses P_{total} for the proposed method to avoid both TNF_1 and TNF_2. High m_f implies high switching losses.

average conduction losses over the fundamental period T can be calculated as:

$$P_D = \frac{1}{T}\int_0^{\frac{T}{2}} (1-\delta(t))\cdot\Big[V_F\cdot i(t) + R_{DT}\cdot i^2(t)\Big]dt$$
$$P_T = \frac{1}{T}\int_0^{\frac{T}{2}} \delta(t)\cdot\Big[V_{CE}\cdot i(t) + R_{TT}\cdot i^2(t)\Big]dt \quad (7)$$

where V_F and V_{CE} are the on-state threshold voltages across the diode and collector-emitter power switch voltage respectively, R_{DT} and R_{TT} is the slope resistance for the diode and power switch respectively. Such parameters are obtained directly from the switch datasheet. $\delta(t)$ is the SPWM duty cycle which is given by $\big(\delta(t) = \frac{1}{2} + \frac{1}{2}M\sin(\omega_o t)\big)$, where M is the amplitude modulation index.

P_{COM} is given by:

$$P_{COM} = \frac{f_{sw}\cdot V_{DC}\cdot \max(i(t))}{V_{cc}\cdot I_{cc}\cdot \pi}\Big(E_{ON}+E_{OFF}\Big) \quad (8)$$

where, f_{sw} is the switching frequency, V_{DC} is the DC bus voltage, E_{ON} and E_{OFF} are the turn-on, turn-off switching energy losses respectively and $\max(i(t))$ is the maximum value of the ac current, V_{cc} and I_{cc} are the test voltage and current respectively.

Fig. 8 shows an estimation of the losses in switches P_{total} for the high power switch whose data are in Table III. P_{total} is calculated by summing eqs. (7) and (8) for both $m_{f,TNF1}$ and $m_{f,TNF2}$. Due to the dependence on f_{sw}, it can be noticed that P_{total} is directly proportional to m_f.

VI. Simulation Results

The system presented in Section III is implemented in Matlab/Simulink. Each module is modeled by standard two axis d-q model of PMSM. For each module the classical FOC is implemented, the machine is vector-controlled to operate in maximum torque-per-ampere (MTPA) conditions.

TABLE III
High Power Switch $GD1400HFT170P2S$ rated data

Collector Emitter Voltage V_{CES} [V]	1700
Collector Current I_{Cn} [A] @ T_c= 100 °C	1400
Turn-on, turn-off switching loss E_{ON}, E_{OFF} [mJ]	502, 618
Diode forward voltage V_F [V] @ I_F=1400A	1.8
Maximum Power Dissipation @ T_j = 175 °C V_F [kW]	9.37
Junction to Case Thermal Resistance	
for IGBT R_{thJC_I} and diodes R_{thJC_D} [K/kW]	16, 33
Case to Heat-sink Thermal Resistance	
for IGBT R_{thCH_I} and diodes R_{thCH_D} [K/kW]	8.9, 18.4

For the purpose of the analysis, the system is accelerated from f_{cut-in} to f_{rated}, despite the slow dynamics of the wind turbine. The angular deflection of all four rotors of the machine is observed. The first considered case is using the proposed method to avoid the excitation of TNF_1, which entitles the excitation of higher modes of vibration.

Fig. 9 shows the effect, due to the excitation of TNF_2, on the angular deflection of the third rotor θ_3 due to the operation with $m_{f,TNF1}$. The maximum deflection due to second mode excitation is shown in Fig. 4 is θ_3. An amplification of θ_3 occurs at the critical frequencies, however it remains small compared to the maximum allowable deflection which can be calculated as:

$$\theta_{max} = \frac{0.8\cdot\sigma_{max}\cdot l_{sh}}{G\cdot R_{ext}} \simeq 4\cdot 10^{-4} \quad [\text{rad}] \quad (9)$$

where, σ_{max} is the maximum allowable stress for steel $\simeq$ 117.7 MPa, G is the torsional modulus of rigidity for steel $\simeq$ 79.3 GPa, l_{sh} and R_{ext} are the length of the shaft between two rotor and the rotor external radius respectively.

Fig. 10 shows the angular deflection of the maximum deflected rotor θ_4 and θ_3 due to the third and fourth mode excitations respectively shown in Fig. 4. Due to the operation with $m_{f,TNF2}$, even if the higher modes are excited, the internal damping of the system is enough to maintain the deflection undetected.

Fig. 11 compares the electromagnetic torque for the operation with $m_{f,TNF1}$ and $m_{f,TNF2}$. As it can be seen, the ripple content for $m_{f,TNF2}$ is much lower.

Since the proposed method mainly affects THD_T and P_{total}, the choice remains related to the application:

- If the internal damping is not high enough, higher $TNFs$ have to be considered. Thus, it will have the priority in choosing the values of m_f;
- THD_T, which is directly proportional to I_h, can also be the defining criterion. As discussed in [9], the higher the current harmonics, the higher the dc bus voltage distortions are. As a result the expected life-time of the capacitor dielectric decreases. In addition, the higher harmonic distortions also affect the quality of the operation, may raise the temperature of the windings increasing the wear-rate of the insulation. This can be achieved by

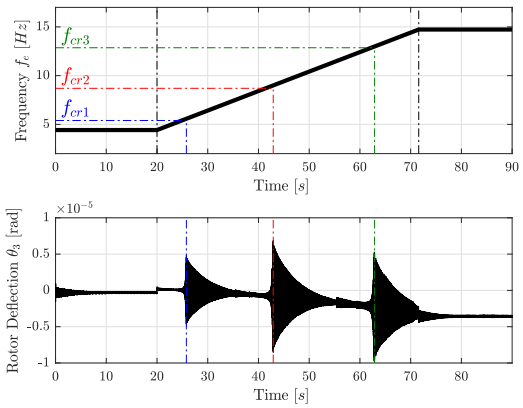

Fig. 9. Operation with $m_{f,TNF1}$ (a) machine frequency f_e during the acceleration from f_{cut-in} to f_{rated}; (b) angular deflection of the third rotor θ_3 being excited by TNF_2. An amplification of the deflection occurs but still remains well away from the maximum deflection θ_{max}.

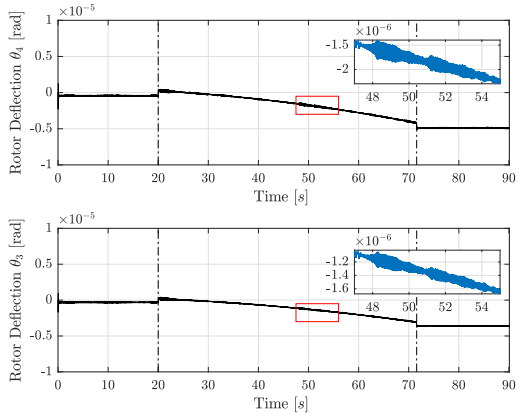

Fig. 10. Operation with $m_{f,TNF2}$ (a) angular deflection of the fourth rotor θ_4 excited by TNF_3; (b) angular deflection of the third rotor θ_4 excited by TNF_4. The deflection is undetected due to the system internal damping.

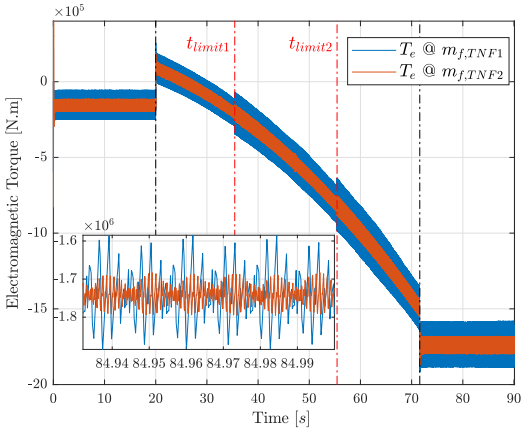

Fig. 11. Electromagnetic torque for the operation under $m_{f,TNF1}$ and $m_{f,TNF2}$ showing the change in m_f at t_{limit1} and t_{limit2} (corresponding to f_{limit1} and f_{limit2}). Also it shows the waveforms for a period at f_{rated}.

the division of the lower frequency portions into several smaller portions changing m_f more frequently in order to keep a maximum limit of THD;

- converter losses P_{total} can be the critical parameter. If the cooling system needs to be upgraded in order to dissipate more power, this implies a defined maximum limit P_{total_m}. Thus, the choice of m_f can be calculated from setting the limit P_{total_m} which can be done by dividing the higher frequency portions into smaller portions.

VII. Conclusion

This paper proposed a practical approach to avoid torsional vibration excitations. This method can be applied for existing applications driven by $SPWM$ modulation. It consists of using a value of m_f high enough to avoid the TNF by the least order torque harmonic $m_f - 3$. In order to limit switching losses, the operating region is divided into several partitions. A criterion to define m_f for each partition that also respects the aforementioned constraint was defined.

The approach was applied on AFPMSG machine consisting of four rotors directly driven by a wind turbine. Such a mechanical assembly has four modes of vibrations. Avoiding torsional excitations from the first mode or from the first and second modes were the only cases considered. An analytical analysis considering torque harmonic distortion THD_T and converter losses was performed for the overall speed range. Matlab/Simulink simulation validated the approach

References

[1] J. Song-Manguelle, C. Sihler, and J. M. Nyobe-Yome, "Modeling of torsional resonances for multi-megawatt drives design," in *2008 IEEE Industry Applications Society Annual Meeting*, Oct 2008, pp. 1–8.

[2] J. Song-Manguelle, J. M. N.-Yome, and G. Ekemb, "Pulsating torques in pwm multi-megawatt drives for torsional analysis of large shafts," *IEEE Transactions on Industry Applications*, vol. 46, no. 1, pp. 130–138, Jan 2010.

[3] M. Bruha and Z. Peroutka, "Torsional vibration in large variable speed drive systems: Origin and mitigation methods," in *2015 17th European Conference on Power Electronics and Applications (EPE'15 ECCE-Europe)*, Sept 2015, pp. 1–10.

[4] F. Fateh, W. N. White, and D. Gruenbacher, "Torsional vibrations mitigation in the drivetrain of dfig-based grid-connected wind turbine," *IEEE Transactions on Industry Applications*, vol. 53, no. 6, pp. 5760–5767, Nov 2017.

[5] J. Song-Manguelle, C. Sihler, and S. Schramm, "A general approach of damping torsional resonance modes in multi-megawatt applications," in *2010 IEEE Energy Conversion Congress and Exposition*, Sept 2010, pp. 772–779.

[6] Z. Q. Zhu and J. H. Leong, "Analysis and mitigation of torsional vibration of pm brushless ac/dc drives with direct torque controller," *IEEE Transactions on Industry Applications*, pp. 1296–1306, July 2012.

[7] A. Di Gerlando, K. ElShawarby, G. M. Foglia, and R. Perini, "Torsional vibration mitigation by harmonic inversion through spwm carrier signal control," in *2018 XIII International Conference on Electrical Machines (ICEM)*, Sep. 2018, pp. 2330–2336.

[8] A. Di Gerlando, K. ElShawarby, G. M. Foglia, M. F. Iacchetti, and R. Perini, "Dc current and torque ripple mitigation in modular pmsg drives for multi-mw wecss with linear pwm inverter modulation," in *2018 XIII International Conference on Electrical Machines (ICEM)*, Sep. 2018, pp. 1458–1464.

[9] A. Carboni, K. El Shawarby, A. Di Gerlando, G. M. Foglia, R. Perini, and E. Ragaini, "Electric stress in power electronics applications," in *2019 XIII IEEE PES anchor conference in Europe (PowerTech), Milan, 2019.*